Protective Effect of Perindopril on Diabetic Retinopathy Is Associated With Decreased Vascular Endothelial Growth Factor–to–Pigment Epithelium–Derived Factor Ratio

Involvement of a Mitochondria–Reactive Oxygen Species Pathway

Zhi Zheng,[1] Haibing Chen,[2] Genjie Ke,[3] Ying Fan,[1] Haidong Zou,[1] Xiaodong Sun,[1] Qing Gu,[1] Xun Xu,[1] and Patrick C.P. Ho[4]

OBJECTIVE—This study aimed to verify whether the decreased vascular endothelial growth factor (VEGF)–to–pigment epithelium–derived factor (PEDF) ratio can serve as an indicator for the protective effect of angiotensin-converting enzyme inhibitors (ACEIs) on diabetic retinopathy (DR) and to investigate the role of mitochondrial reactive oxygen species (ROS) in the downregulated VEGF-to-PEDF ratio.

RESEARCH DESIGN AND METHODS—Diabetic rats and control animals were randomly assigned to receive perindopril or vehicle for 24 weeks, and bovine retinal capillary endothelial cells (BRECs) were incubated with normal or high glucose with or without perindopril. VEGF, PEDF, PPARγ, and uncoupling protein-2 (UCP-2) in the rat retinas or BREC extracts were examined by Western blotting and real-time RT-PCR. The levels of VEGF and PEDF in cell culture media were examined by ELISA. Mitochondrial membrane potential ($\Delta\psi m$) and ROS production were assayed using JC-1 or CM-H2DCFDA.

RESULTS—The VEGF-to-PEDF ratio was increased in the retina of diabetic rats; perindopril lowered the increased VEGF-to-PEDF ratio in diabetic rats and ameliorated the retinal damage. In BRECs, perindopril lowered the hyperglycemia-induced elevation of VEGF-to-PEDF ratio by reducing mitochondrial ROS. We found the decreased ROS production was a result of perindopril-induced upregulation of PPARγ and UCP-2 expression and the subsequent decrease of $\Delta\psi m$.

CONCLUSIONS—It is concluded that the protective effect of ACEI on DR is associated with a decreased VEGF-to-PEDF ratio, which involves the mitochondria-ROS pathway through PPARγ-mediated changes of UCP-2. This study paves a way for future application of ACEI in treatment of DR. ***Diabetes*** **58:954–964, 2009**

Diabetic retinopathy (DR) is a major cause of blindness in the working-age population in developed countries (1), and to search for effective treatment and prevention measures has long been a focus of study. The EUCLID Study Group reported that the antihypertensive drug lisinopril, an angiotensin-converting enzyme inhibitor (ACEI), reduced the risk of retinopathy progression by ~50% in patients with type 1 diabetes, thus greatly reducing the possibility of proliferative diabetic retinopathy (PDR) (2). Recently, another ACEI, perindopril, has been found capable of improving the visual functions, retinal electrogenesis, and disturbed blood–retinal barrier in patients with preproliferative diabetic retinopathy (DR) (3). Studies also indicated that the protective effect of ACEI on DR-related damage was associated with a decreased expression of vascular endothelial growth factor (VEGF) in the retina (4,5), and VEGF was involved in vascular leakage and angiogenesis in DR (6). Our previous study demonstrated that ACEI inhibited retinal VEGF expression independent of their antihypertensive actions (7). The detailed mechanism by which ACEI counteracts hyperglycemia-induced VEGF upregulation, however, remains to be further clarified.

In addition to VEGF, pigment epithelium–derived factor (PEDF), a potent inhibitor of angiogenesis, has been found to be involved in the pathogenesis of PDR (8,9). It is well known that there are quite a few stimulators and inhibitors of angiogenesis in the eye; among them, VEGF has been identified as a primary angiogenic stimulator (10) and PEDF as a major angiogenic inhibitor (9). The time course of the VEGF-to-PEDF ratio change correlated with the development and progression of retinal neovascularization. The VEGF-to-PEDF ratio represented a dynamic balance between angiogenic stimulators and inhibitors; and disturbance of the balance played a key role in the pathogenesis of DR (11–13). In vitro study revealed that lowering of the VEGF-to-PEDF mRNA ratio could inhibit the migration of uveal melanoma cells (14). Despite these

From the [1]Department of Ophthalmology, First People's Hospital of Shanghai, Shanghai Jiaotong University, Shanghai, China; the [2]Department of Endocrinology and Metabolism, the Sixth People's Hospital of Shanghai Affiliated to Shanghai Jiaotong University, Shanghai, China; the [3]Department of Ophthalmology, Anhui Provincial Hospital, Hefei, China; and [4]Hong Kong Eye Associates, Hong Kong, China.

Corresponding author: Xun Xu, xuxun60@yahoo.com.cn.

Received 26 October 2007 and accepted 15 January 2009.

Published ahead of print at http://diabetes.diabetesjournals.org on 2 February 2009. DOI: 10.2337/db07-1524.

Z.Z. and H.C. contributed equally to this work.

findings, the influence of ACEI on the VEGF-to-PEDF ratio remains unknown.

Currently, the specific mechanism of diabetic microangiopathy is not completely understood. Recently, a unifying hypothesis has been proposed whereby production of mitochondrial reactive oxygen species (ROS) in response to chronic hyperglycemia might be the key initiator for all of the four pathogenic pathways: the increased polyol pathway flux, increased formation of advanced glycation end products, activation of protein kinase C, and increased hexosamine pathway flux (15–17). This postulate emphasized the important role of the increased mitochondrion ROS production in diabetes complications, including retinopathy. Therefore, mitochondrial ROS may serve as an important target for DR treatment. ACEI was demonstrated to attenuate ROS generation in the heart and aorta of diabetic rats and prevent morphological changes (cardiomyocyte hypertrophy and perivascular fibrosis) (18). It can be deduced that the protective effect of ACEI is associated with repression of oxidative stress.

The aim of the present study is to verify whether the decreased VEGF-to-PEDF ratio can serve as an indicator for the protective effect of ACEI on DR and to investigate the role of ROS in the downregulation of the VEGF-to-PEDF ratio and the related mechanism. We found that the decreased VEGF-to-PEDF ratio was associated with the protective effect of ACEI on DR, and the decrease of VEGF-to-PEDF ratio was caused by reduced mitochondrial ROS production; our study further indicated that the reduced ROS production was a result of ACEI-induced upregulation of PPARγ and uncoupling protein-2 (UCP-2) expression. Our findings indicate that ACEI possesses a great potential for treatment of DR.

RESEARCH DESIGN AND METHODS

All experiments in this study comply with the requirements of the Association for Research in Vision and Ophthalmology statement with regard to the "Use of Animals in Ophthalmic and Vision Research." All chemicals were reagent grade quality and were purchased from Sigma Chemicals (St. Louis, MO) unless stated otherwise.

Animals. Eight-week-old male Sprague-Dawley rats weighing ~200 g (Shanghai Laboratory Animal Center, Chinese Academy of Sciences) were randomly assigned to receive either 60 mg/kg STZ intraperitoneally or citrate buffer alone. Rats were categorized as diabetic when the blood glucose exceeded 16.7 mmol/l at 48 h after STZ administration. One week after the injection of STZ, diabetic rats were randomly assigned to groups receiving either 2 mg · kg^{-1} · day^{-1} perindopril (Servier, Tianjin, China) by drinking water for 24 weeks or no treatment at all. Age-matched rats receiving no STZ served as controls. All rats had free access to standard rat food and drinking water. Diabetic rats received subcutaneous insulin (Humulin-N; Eli Lilly & Co., Indianapolis, IN) twice a week to maintain body weight and maximize survival rate (0–4 units).

Cell culture. The primary culture of bovine retinal capillary endothelial cells (BRECs) was done as described in our previous study (19). The endothelial cells of three to four passages were used in the following experiments. In each case, the confluent-cultured BRECs were maintained in free-serum DMEM. The cells were exposed to normal glucose (5 mmol/l), normal glucose plus mannitol (25 mmol/l), normal glucose plus perindopril (10 μmol/l), normal glucose plus H_2O_2 (500 μmol/l), high glucose (30 mmol/l), high glucose plus perindopril (10 μmol/l), high glucose plus ROS scavenger N-acetylcysteine (NAC; 10 mmol/l), high glucose plus perindopril plus NAC, or high glucose plus perindopril plus NAC plus GW9662 (an inhibitor of PPARγ; 20 μmol/l).

Uncoupling protein-2 antisense oligonucleotide treatment. UCP-2 antisense oligonucleotide synthesis and treatment were conducted as described previously (20). UCP-2 antisense oligonucleotide sequence was 5′-TGAGATCTGCAATACA-3′, and the corresponding sense oligonucleotide sequence was 5′-TGTATTGCAGATCTCA-3′. After 24 h, the medium was removed, free-serum DMEM in high glucose was added, and the cells were allowed to recover for 30 min. Then BRECs were washed once with free-serum DMEM and exposed to either normal glucose (5 mmol/l) or high glucose (30 mmol/l) for 24 h.

Retinal digest procedures. Harvested eyes were immediately placed in 4% buffered paraformaldehyde for 24 h. Retinal trypsin digestion was performed according to the method described by Cogan and associates (21). Preparations of retinal vascular networks were placed onto polylysine-coated glass slides in distilled water and then dried. The preparations were stored at −20°C until periodic acid Schiff (PAS) and hematoxylin staining. The capillary network was investigated to determine the numbers of pericytes and acellular capillaries as previously described (22).

Transmission electron microscopy. Tissue processing, electron microscopy, morphometric measurements (retinal capillary basement membrane thickness [BMT]), and statistics were performed as detailed in our previous study (6). Enucleated eyes were fixed in 2.5% glutaraldehyde in 0.1 mol/l cacodylate buffer (pH 7.4) containing 0.2% tannic acid, washed in the same buffer, and postfixed in 0.5% osmium tetroxide. Tissue sections were block stained with uranyl acetate, lead stained, dehydrated through a graded series of ethanol, and embedded in epon. One-micrometer-thick sections were examined with a JEM-1200EX transmission electron microscope (JEOL, Akishima, Japan). Computer-assisted morphometric measurements (The Image Center of Beijing University of Aeronautics & Astronautics, Beijing, China) were done on electron micrographs taken from 12 randomly selected capillaries of the outer plexiform layer from four different tissue blocks of the same retina. Only cross-sectioned capillaries were considered. A total of 96 capillaries were evaluated in each experiment group.

Measurement of ROS. ROS production in the cells was assessed using the fluorescent probe 5-(and-6)-chloromethyl-2′,7′-dichlorodihydrofluorescein diacetate acetyl ester (CM-H2DCFDA; Molecular Probes, Eugene, OR). CM-H2DCFDA (λ_{ex}, 488 nm and λ_{em}, 520 nm) is a cell-permeable indicator of ROS that remains nonfluorescent until acetate groups are removed (H2DCF) by intracellular esterases and oxidation occurs within the cells. Two hundred microliters of the cell suspension were loaded into the wells of a FluoroNunc 96-well polystyrene plate together with CM-H2DCFDA (10 μmol/l) for 45 min at 37°C. Intracellular ROS production was calculated using an H_2O_2 standard curve (10–200 nmol/ml). Retinal mitochondria ROS production was detected as described by Benani et al. (23). Retinal tissues were harvested in cold-buffered medium (5 mmol/l HEPES in PBS) and immediately frozen in liquid nitrogen to improve the following probe diffusion. After rapid thawing, medium was discarded. Samples were exposed to 8 μmol/l CM-H2DCFDA dissolved in 400 μl fresh medium and were incubated at 37°C for 30 min under agitation. Medium was then removed, and samples were further incubated in a lysis buffer (0.1% SDS, Tris-HCl, pH 7.4) for 15 min at 4°C. After homogenization, samples were centrifuged at 6,000*g* for 20 min at 4°C. Supernatants were collected and subjected to fluorescence analysis as stated previously.

Mitochondrial membrane potential. 5,5′,6,6′-tetrachloro1,1′,3,3′-tetraethylbenzimidazolylcarbocyanine iodide (JC-1; Molecular Probes) is a potentiometric dye that exhibits membrane potential–dependent loss as J-aggregates (polarized mitochondria) that are converted to JC-1 monomers (depolarized mitochondria) as indicated by the fluorescence emission shift from red to green. Mitochondrial depolarization is indicated by an increase in the green/red fluorescence intensity ratio. Mitochondrial membrane potential ($\Delta\psi m$) measurement in BRECs or retinal tissues was performed using flow cytometry (Coulter Epics XL; Beckman-Coulter) as described in our previous study and by Hassouna and associates (19,24).

Real-time RT-PCR. Total RNA was extracted from rat retinal tissue and BRECs using TRIZOL reagent (Invitrogen Life Technologies, Gaithersburg, MD) and stored at −80°C. The DyNAmo Flash SYBR Green qPCR kit (Finnzymes Oy, Espoo, Finland) was used according to the manufacturer's instructions. The primer sequences (sense/antisense) used were as follows: PEDF, 5′-CAGAAGA ACCTCAAGAGTGCC-3′/5′-CTTCATCCAAGTAGAAATCC-3′; VEGF, 5′-GCG-GGCTGCTGCAATG-3′/5′-TGCAACGCGAGTCTGTGTTT-3′; UCP-2, 5′-TCTGA CCATGGTGCGTACTGA-3′/5′-GACAATGGCATTACGAGCAAC-3′; PPARγ1, 5′-TTCTGACAGGACTGTGTGACAG-3′/5′-ATAAGGTGGAGATGCAGGTTC-3′; PPARγ2, 5′-GCTGTTATGGGTGAAACTCTG-3′/5′-ATAAGGTGGAGATGCAGG TTC-3′; and β-actin, 5′-GCACCGCAAATGCTTCTA-3′/5′-GGTCTTTACGGATG TCAACG-3′. The specificity of the amplification product was determined by a melting curve analysis. Standard curves were generated for the expression of each gene by preparing serial dilutions with known quantities of each cDNA template. Relative quantification of the signals was performed by normalizing the signals of different genes with the β-actin signal. Signal intensities in the control lanes were arbitrarily assigned a value of 1.0.

Western blotting. Retinas were removed rapidly and frozen in liquid nitrogen. The frozen tissues were homogenized with lysis buffer (50 mmol/l Tris-HCl [pH 7.4], 10% glycerol, 2 mmol/l EDTA, 150 mmol/l NaCl, 1 mmol/l $MgCl_2$, 50 mmol/l glycerophosphate, 2 mmol/l Na_3VO_4, 20 mmol/l NaF, 1 mmol/l phenylmethylsulfonylfluoride, 10 μg/ml leupeptin, 10 μg/ml aprotinin, and 1% Nonidet P-40) and were centrifuged at 12,000 rpm for 15 min at 4°C.

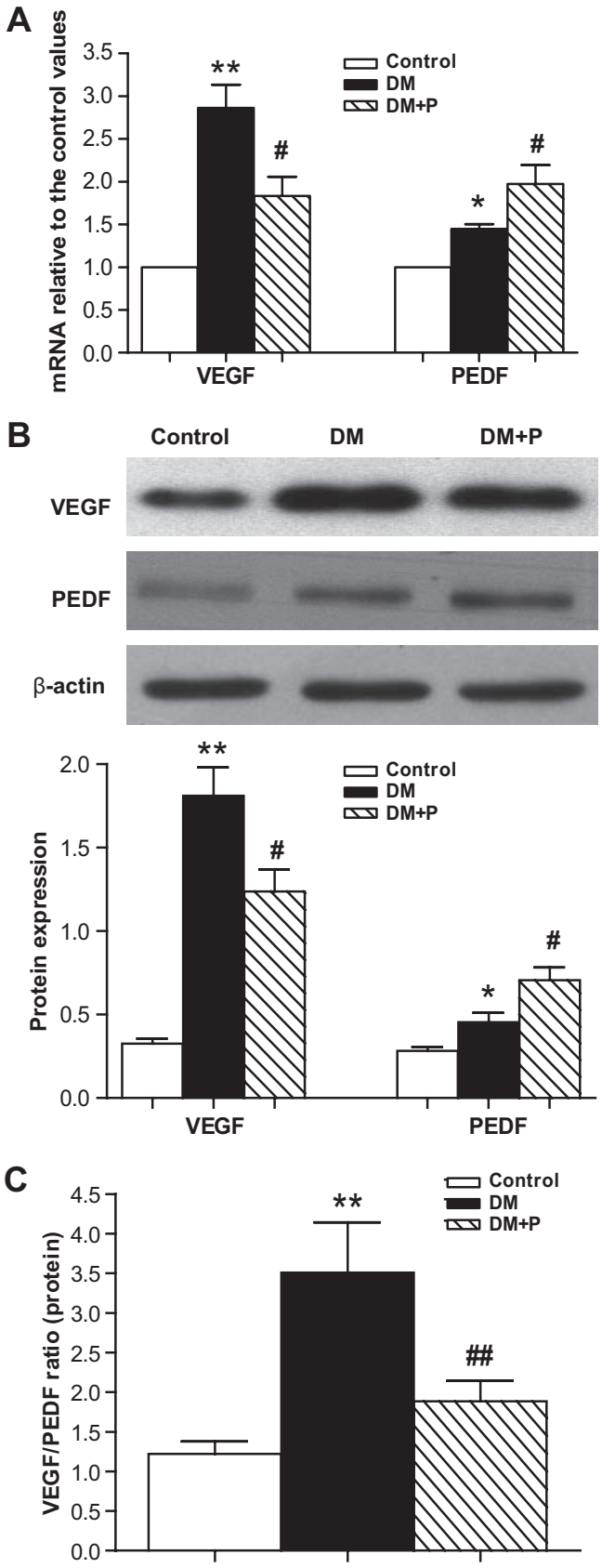

FIG. 1. Changes of retinal VEGF and pigment epithelium-derived factor (PEDF) levels in the control rats (control), diabetic rats (DM), and diabetic rats treated with perindopril (DM + P). *A*: Real-time RT-PCR determination of VEGF and PEDF mRNAs relative to the control values. *B*: Western blotting analysis of VEGF and PEDF protein expression in the three groups. Equal protein loading was confirmed with the β-actin antibody. *C*: VEGF-to-PEDF ratios (protein) in the three groups. Levels of VEGF and PEDF were first normalized by β-actin at each time point. The normalized VEGF level was divided by the corresponding PEDF levels for VEGF-to-PEDF ratio. Data are means ± SD from eight rats per group, and the experiments were repeated independently at least three times with similar results. **$P < 0.01$ versus control, #$P < 0.05$ versus DM.

BREC extracts were prepared with the same lysis buffer. The protein concentrations in the supernatants were measured using the Bio-Rad DC protein assay. Fifty micrograms of protein from each sample (retinas or BRECs) were subjected to SDS-PAGE using a Bio-Rad miniature slab gel apparatus and electrophoretically transferred onto a nitrocellulose sheet. The sheet was blocked in 5% nonfat dried milk solution and incubated overnight with partially purified goat anti-PEDF (Chemicon International) monoclonal antibody, mouse anti-VEGF (Chemicon, Temecula, CA) monoclonal antibody, rabbit anti–UCP-2 polyclonal antibody (Merck & Co.), and rabbit anti-PPARγ polyclonal antibody (MILLIPORE). β-Actin (monoclonal anti-β-actin; Sigma Chemical) expression was used as an internal control.

ELISA. The PEDF concentrations in cell media were measured using a 2-antibody sandwich ELISA. Assays were performed in 96-well immunoplates (Chemicon International). VEGF ELISA was performed using a Quantikine VEGF assay kit (R & D Systems) to quantify the levels of VEGF in cell media. Serial dilutions of recombinant human VEGF and PEDF were included in all assays to serve as standards.

The experimental data were expressed as means ± SD. Group means were compared by a one-way ANOVA using the GraphPad Prism 4.0 software system (GraphPad, San Diego, CA) and the statistical software program SPSS13.0 for Windows (Chicago, IL). Pearson correlation tests were also performed. P values <0.05 were considered significant in all cases.

RESULTS

Perindopril inhibited the increase of VEGF-to-PEDF ratio and attenuated retinal damages in diabetic rats. The retinal expression of PEDF and VEGF was significantly increased in the diabetic rats compared with that in the nondiabetic rats at both mRNA and protein levels, whereas the VEGF-to-PEDF ratio was still significantly increased in diabetic rats compared with that in the nondiabetic rats ($P < 0.01$) (Fig. 1*A–C*). Pathological damage of the retina occurred in diabetic rats at an early stage (Fig. 2*A–C*). Compared with the nondiabetic rats, the number of pericytes in the retinas of diabetic rats was significantly reduced ($P < 0.01$), and the number of acellular capillary segments and BMT were significantly increased ($P < 0.01$) (Fig. 2*D–F*). Statistical analysis showed that the VEGF-to-PEDF ratio was negatively correlated with the number of pericytes and positively correlated with acellular capillary segments and BMT before and after perindopril treatment (Table 1). Perindopril significantly inhibited the increase of VEGF-to-PEDF ratio in diabetic rats (Fig. 1*A–C*) and attenuated the damages to the retinas (Fig. 2*A–F*), and the decrease of the VEGF-to-PEDF ratio was significantly correlated with the attenuation of retinal damage (Table 1). In addition, we found that the nonfasting blood glucose was markedly higher in the diabetic rats than in the nondiabetic rats (28.5 ± 4.3 mmol/l versus 4.3 ± 0.5 mmol/l, $P < 0.01$), and perindopril showed no effect on hyperglycemia in diabetic rats (27.3 ± 3.8 mmol/l versus 28.5 ± 4.3 mmol/l, $P > 0.05$). The body weights of diabetic rats and perindopril-treated diabetic rats were significantly lower than that of nondiabetic rats (377 ± 28 g or 392 ± 36 g versus 594 ± 45 g, $P < 0.05$).

Decreased VEGF-to-PEDF ratio is associated with reduced mitochondrial ROS generation after perindopril treatment. Compared with nondiabetic rats, the production of mitochondrial ROS, Δψm, and the expression of UCP-2 and PPARγ protein were significantly increased in the retinas of diabetic rats ($P < 0.01$).

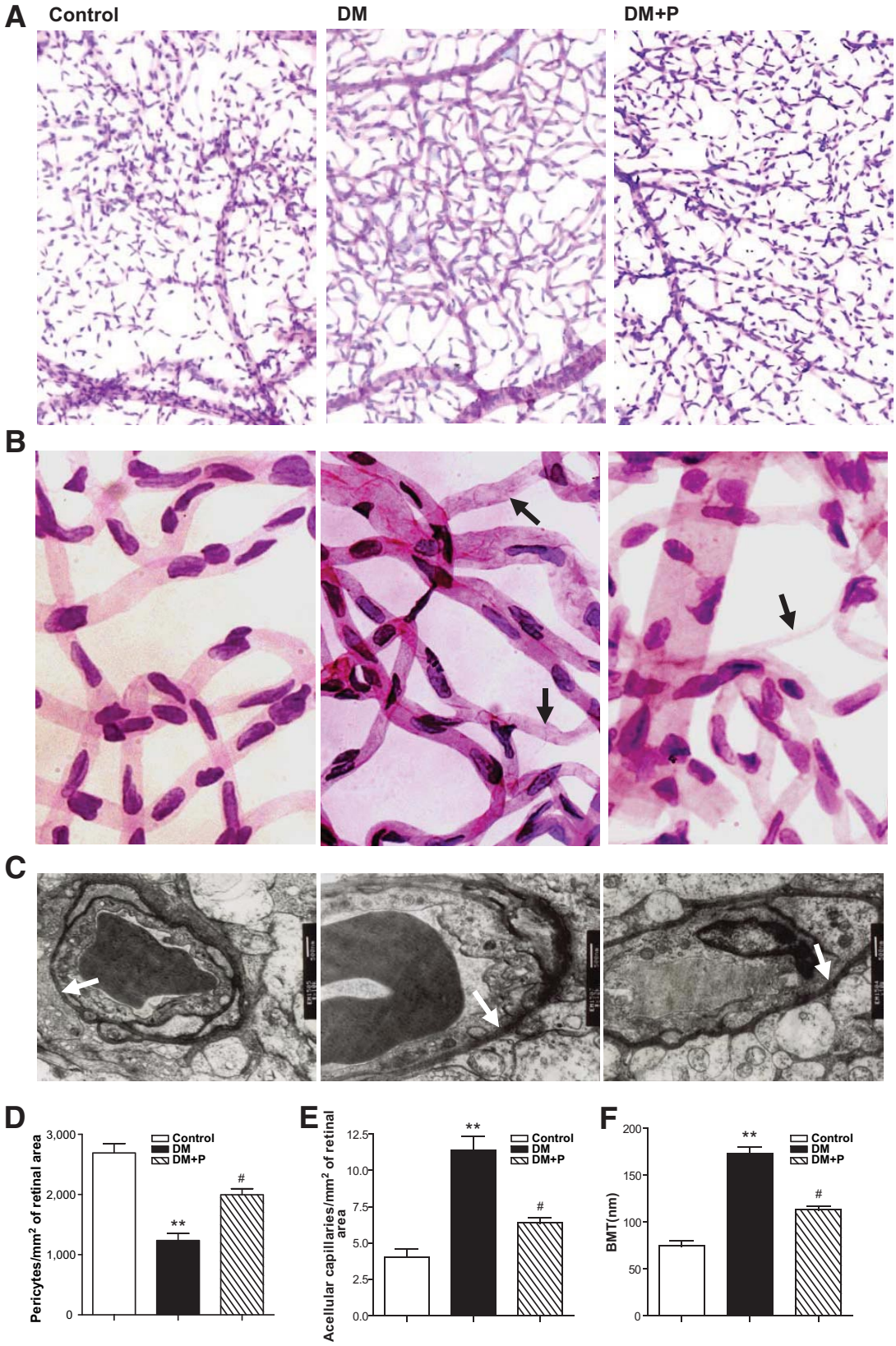

FIG. 2. Observation of early retinal histopathological lesions in the control, diabetic rats (DM), and diabetic rats treated with perindopril (DM + P) groups. *A* and *B*: Low- and high-magnification (×50 and ×400) photomicrographs of trypsin-digested retinal blood vessels obtained from the three groups. All preparations were stained with PAS and hematoxylin; *arrowheads* indicate acellular capillary. *C*: Transmission electron micrograph of a capillary from outer plexiform layer of rat retinas in the three groups. *Arrows* denote the segment of the outer capillary basement membrane between the endothelial cells and glia limitans, which was used to measure basement membrane width (original magnification ×9,000). *D–F*: Determination of pericyte/mm² of capillary area (*D*), acellular capillary segment/mm² in the retinal vessels (*E*), and retinal capillary basement membrane thickness (BMT, nm) (*F*) in the three groups. Data are means ± SD from eight rats per group, and the experiments were repeated independently at least three times with similar results. **$P < 0.01$ versus control, #$P < 0.05$ versus DM. (A high-quality digital representation of this figure is available in the online issue.)

TABLE 1
Correlation analysis between retinal VEGF-to-PEDF ratio and early histopathological lesions in diabetic rats with or without perindopril treatment ($n = 8$)

	r	P
DM		
Number of pericytes	−0.808	0.015
Number of acellular vessels	0.863	0.006
BMT	0.796	0.018
DM + P		
Number of pericytes	−0.773	0.025
Number of acellular vessels	0.923	0.001
BMT	0.800	0.017

DM, diabetic rats; DM + P, diabetic rats treated with perindopril.

Perindopril treatment reduced ROS production and Δψm but further upregulated the expression of UCP-2 and PPARγ protein (Fig. 3*A–D*). Pearson correlation analysis indicated that the decrease of the VEGF-to-PEDF ratio was correlated with the reduction of mitochondrial ROS in the perindopril-treated group (Fig. 3*B*) ($r = 0.749$, $P = 0.032$). In addition, statistical analysis showed that there was a correlation between mitochondrial ROS and Δψm ($r = 0.902$, P = 0.003), between Δψm and UCP-2 ($r = 0.823$, $P = 0.012$), and between UCP-2 and PPARγ levels ($r = 0.887$, $P = 0.005$) in the perindopril-treated group.

Perindopril inhibited hyperglycemia-induced elevation of VEGF-to-PEDF ratio through reducing ROS production. To understand the mechanism underling the inhibitory effect of perindopril on the VEGF-to-PEDF ratio, an in vitro study was performed with BRECs. Exposure of BRECs to high glucose increased ROS production, upregulated VEGF mRNA and protein in cell extracts or media, downregulated PEDF mRNA and protein in cell extracts or media, and elevated the VEGF-to-PEDF ratio (protein in cell extracts or media), whereas these changes were significantly inhibited by 10 μmol/l perindopril (Fig. 4*A–F*). Our results also showed that NAC, an ROS scavenger, arrested the elevation of the VEGF-to-PEDF ratio (upregulating VEGF and downregulating PEDF). We also found that incubation with H_2O_2 upregulated VEGF, downregulated PEDF, and elevated VEGF/PEDF ratio in BREC extracts or media (Fig.

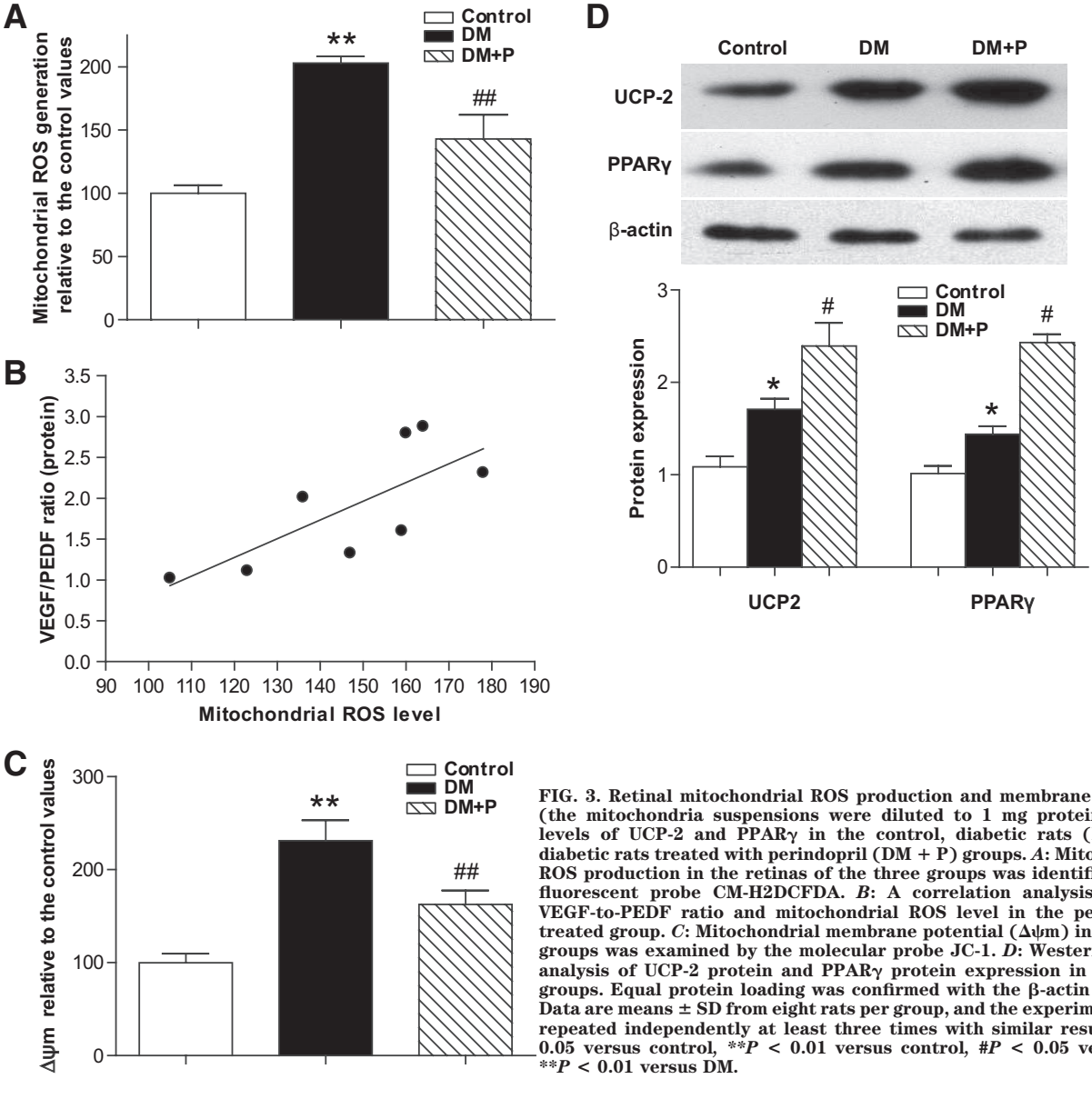

FIG. 3. Retinal mitochondrial ROS production and membrane potential (the mitochondria suspensions were diluted to 1 mg protein/ml) and levels of UCP-2 and PPARγ in the control, diabetic rats (DM), and diabetic rats treated with perindopril (DM + P) groups. *A*: Mitochondrial ROS production in the retinas of the three groups was identified by the fluorescent probe CM-H2DCFDA. *B*: A correlation analysis between VEGF-to-PEDF ratio and mitochondrial ROS level in the perindopril-treated group. *C*: Mitochondrial membrane potential (Δψm) in the three groups was examined by the molecular probe JC-1. *D*: Western blotting analysis of UCP-2 protein and PPARγ protein expression in the three groups. Equal protein loading was confirmed with the β-actin antibody. Data are means ± SD from eight rats per group, and the experiments were repeated independently at least three times with similar results. *P < 0.05 versus control, **P < 0.01 versus control, #P < 0.05 versus DM, **P < 0.01 versus DM.

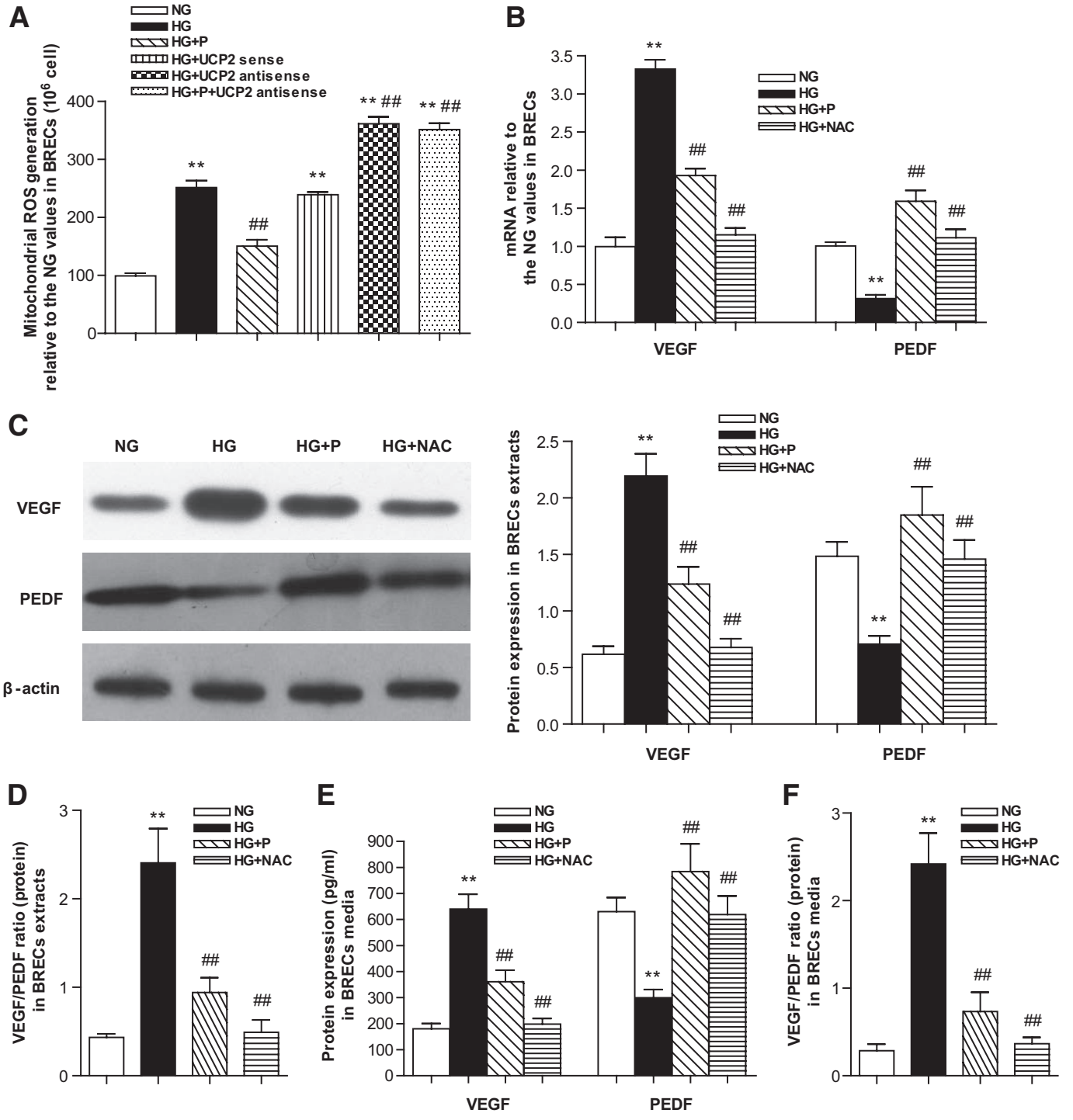

FIG. 4. ROS production and levels of VEGF and PEDF in BRECs exposed to normal glucose (NG) or high glucose (HG). *A*: Intracellular ROS production was determined by the fluorescent probe CM-H2DCFDA in BRECs exposed to NG, HG, HG + perindopril (HG + P), HG + UCP-2 sense, HG + UCP-2 antisense, or HG + P + UCP-2 antisense for 24 h. *B*: VEGF and PEDF mRNAs in BRECs were determined by real-time RT-PCR in NG, HG, HG + P, or HG with NAC (HG + NAC) for 72 h. Results are expressed relative to the NG values. *C* and *E*: Western blotting analysis of VEGF and PEDF protein expression in BREC extracts (*C*) and ELISA analysis of VEGF and PEDF protein expression in BREC media (*E*) in the four groups. *D* and *F*: VEGF-to-PEDF ratios (protein in BRECs extracts [*D*] and in BREC media [*F*]) in the four groups. Levels of VEGF and PEDF were first normalized by β-actin at each time point in Western blotting; the normalized VEGF level was divided by the corresponding PEDF levels for calculation of VEGF-to-PEDF ratio. Data are means ± SD from nine cells per group, and the experiments were repeated independently at least three times (real-time RT-PCR and Western blotting) or two times (ELISA) with similar results. ***P* < 0.01 versus NG, ##*P* < 0.01 versus HG.

5*A–F*). The effect of H_2O_2 on VEGF-to-PEDF ratio was time- and dose-dependent (data not shown). To rule out the influence of osmolarity on the ratio, mannitol was used to treat the cells, and the results showed that mannitol had no effect on the VEGF-to-PEDF ratio (data not shown).

Perindopril reduced ROS production through upregulating PPARγ and UCP-2 and downregulating mitochondrial membrane potential. UCP-2 expression has been reported to be associated with ROS generation (25), and PPARγ has been shown to modulate the transcription activities of genes involved in energy metabolism,

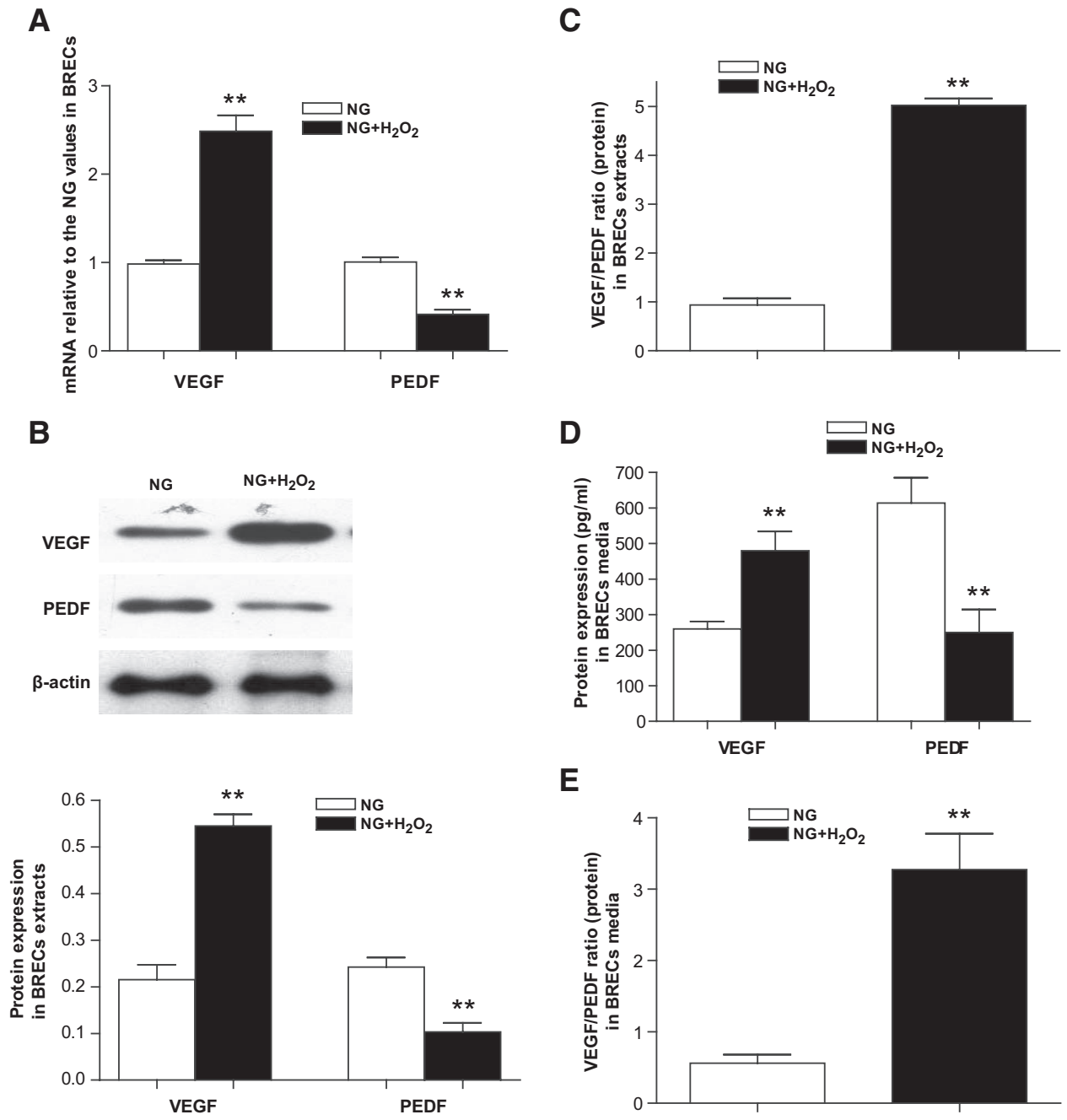

FIG. 5. Levels of VEGF and PEDF in BRECs exposed to normal glucose (NG) or NG + H_2O_2. *A*: VEGF and PEDF mRNAs in BRECs were determined by real-time RT-PCR in the control group and the H_2O_2-treated group. Results are expressed as relative to the NG values. *B* and *D*: Western blotting analysis of VEGF and PEDF protein expression in BREC extracts (*B*) and ELISA analysis of VEGF and PEDF protein expression in BREC media (*D*) in the two groups. *C* and *E*: The VEGF-to-PEDF ratios (protein in BRECs extracts [*C*] and in BREC media [*E*]) in the two groups. Data are means ± SD from nine cells per group, and the experiments were repeated independently at least three times (real-time RT-PCR and Western blotting) or two times (ELISA) with similar results. **$P < 0.01$ versus NG.

including the mitochondrial uncoupling proteins, UCP-1, UCP-2, and UCP-3 (26). To investigate the mechanism by which perindopril reduces ROS production, we examined the mRNA and protein expression of UCP-2 and PPARγ in BRECs exposed to normal and high glucose. We found that the mitochondrial membrane was hyperpolarized under high glucose conditions and the production of ROS was increased; the production of ROS was positively correlated with Δψm ($r = 0.779$, $P = 0.023$); we also found that perindopril significantly decreased hyperglycemia-induced mitochondrial membrane hyperpolarization and the subsequent increased ROS production (Figs. 4*A* and 6*A* and *B*). We found that hyperglycemia induced upregulation of UCP-2 mRNA and protein; perindopril also upregulated UCP-2 expression in BRECs exposed to normal or high glucose with or without NAC (Fig. 6*C* and *D*). Incubation with UCP-2 antisense oligonucleotide greatly enhanced the hyperglycemia-induced Δψm and ROS production, whereas it blocked the inhibitory effect of perindopril on the Δψm and ROS production (Figs. 4*A* and 6*A* and *B*). In addition, as shown in Fig. 7*A–C*, hyperglycemia increased the expression of PPARγ1 and PPARγ2 mRNA and PPARγ protein; perindopril could upregulate their expression under normal conditions

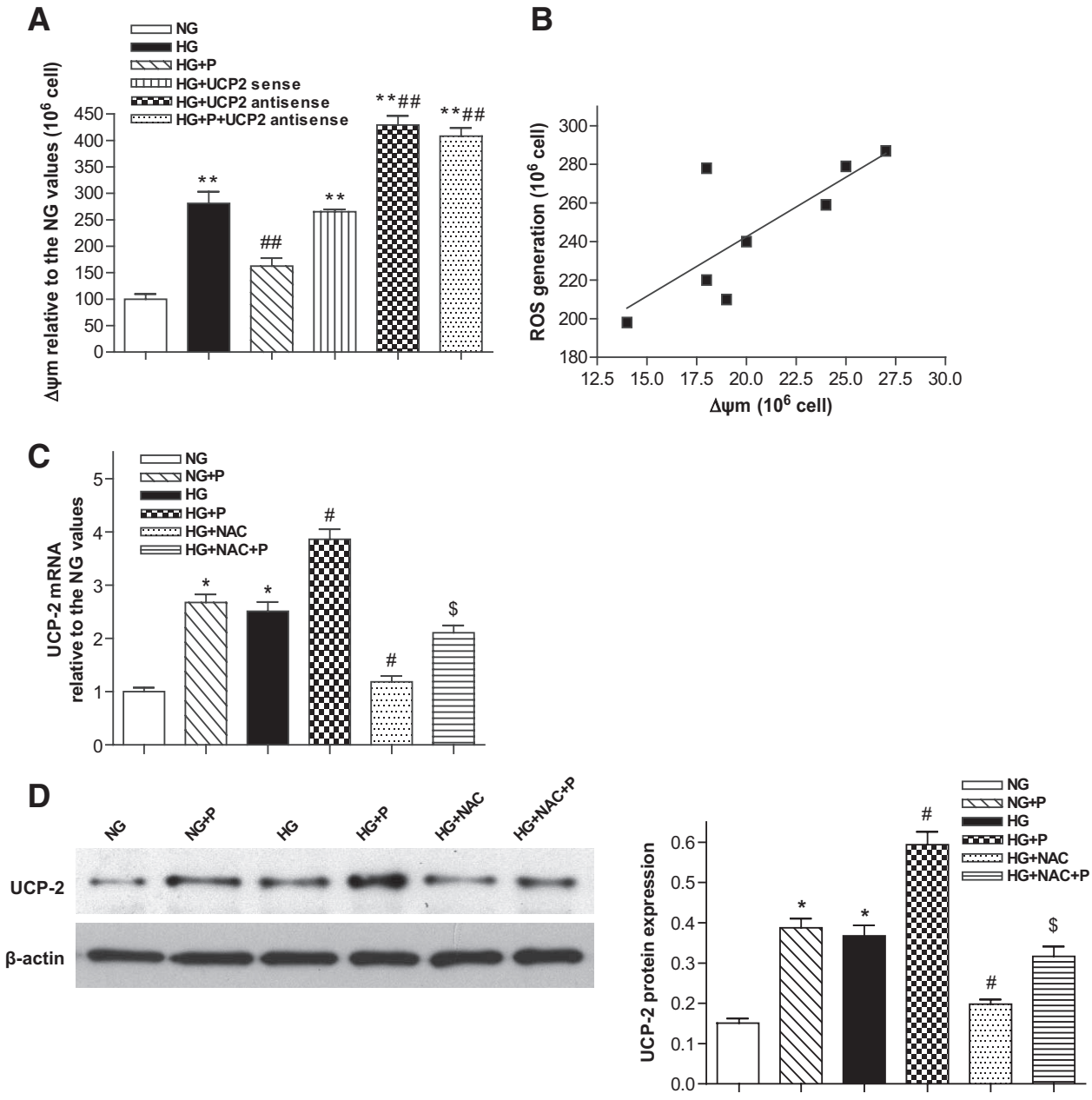

FIG. 6. Mitochondrial membrane potential (Δψm) and UCP-2 level in BRECs. *A*: Δψm in BRECs exposed to normal glucose (NG), high glucose (HG), HG + perindopril (P), HG + UCP-2 sense, HG + UCP-2 antisense, and HG + P + UCP-2 antisense for 24 h was examined by the molecular probe JC-1. *B*: A correlation analysis between intracellular ROS production and Δψm level in BRECs exposed to HG. *C*: UCP-2 mRNAs in BRECs exposed to NG, NG plus perindopril (NG + P), HG, HG plus perindopril (HG + P), HG plus NAC (HG + NAC), and HG plus NAC and perindopril (HG + NAC+ P) were determined by real-time RT-PCR. Results are expressed relative to the NG values. *D*: Western blotting analysis of UCP-2 protein expression in BRECs in NG, NG + P, HG, HG + P, HG + NAC, and HG + NAC + P groups. Equal protein loading was confirmed with the β-actin antibody. Data are means ± SD from nine cells per group, and the experiments were repeated independently at least three times with similar results. *$P < 0.05$ versus NG, **$P < 0.01$ versus NG, #$P < 0.05$ versus HG, ##$P < 0.01$ versus HG, $$P < 0.05$ versus HG + NAC.

and further upregulate their expression under hyperglycemia conditions. We also found that high glucose combined with GW9662, an inhibitor of PPARγ, inhibited the upregulation of UCP-2 in BRECs; besides, GW9662 blocked the upregulating effect of perindopril on UCP-2 (Fig. 7*A*–*C*).

DISCUSSION

Recently, the protective effect of ACEI on DR has increasingly become a focus of study (2–6). We observed the changes of the VEGF-to-PEDF ratio in the rat retinal tissues and BRECs in the presence of normal or high glucose; we also observed the effect of perindopril on changes of the VEGF/PEDF ratio in diabetic rats and in BRECs exposed to high glucose. We confirmed that ACEI exerted a protective effect on DR (2–5,27,28), and for the first time, we found that this protective effect was associated with a decreased VEGF-to-PEDF ratio (downregulating VEGF and upregulating PEDF). We found the decreased VEGF-to-PEDF ratio was a result of reduced mitochondrial ROS production, and the reduced ROS production was attributable to decreased Δψm, which was a result of ACEI-induced upregulation of PPARγ and UCP-2 expression.

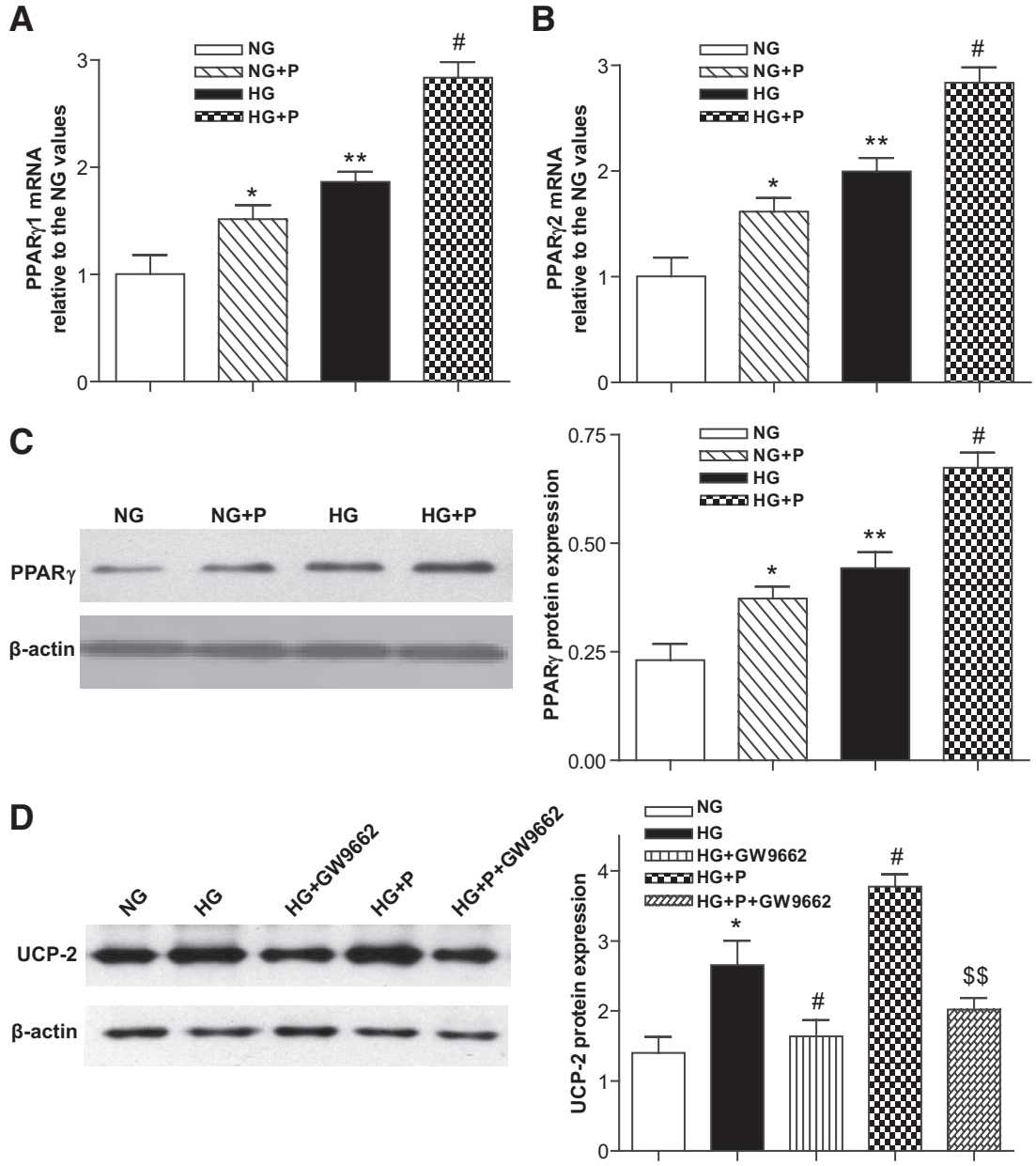

FIG. 7. Levels of PPARγ and UCP-2 in BRECs. *A* and *B*: PPARγ1 (*A*) and PPARγ2 (*B*) mRNAs in BRECs were determined by real-time RT-PCR in normal glucose (NG), NG + perindopril (P), high glucose (HG), and HG + P for 24 h. Results are expressed relative to the NG values. *C*: Western blotting analysis of PPARγ protein expression in the four groups. *D*: Western blotting analysis of UCP-2 protein expression in NG, HG, HG with GW9662 (HG + GW9662), HG + P, and HG plus P and GW9662 (HG + P + GW9662) groups. Equal protein loading was confirmed with the β-actin antibody. Data are means ± SD from nine cells per group, and the experiments were repeated independently at least three times with similar results. *$P < 0.05$ versus NG, **$P < 0.01$ versus NG, #$P < 0.05$ versus HG, $$$P < 0.01$ versus HG + P.

We found that VEGF was upregulated and PEDF was downregulated in the vitreous of patients with PDR, which subsequently elevated the VEGF-to-PEDF ratio and was accompanied by retinal neovascularization (data not shown), whereas in diabetic Sprague-Dawley rats, both VEGF and PEDF were upregulated. (A similar result was also noticed in a study with spontaneously diabetic Torii rats, an animal model of type 2 diabetes [29].) Nevertheless, as a result of even more upregulation of VEGF, the VEGF/PEDF ratio was still significantly elevated compared with that of the controls; the elevation was also accompanied by early vascular damages; and a significant correlation was found between the severity of damage and the VEGF/PEDF ratio. In this study, we found that ACEI perindopril downregulated VEGF and upregulated PEDF, which subsequently resulted in a lowered VEGF-to-PEDF ratio and relieved vascular damage in the retina of diabetic rats; and the lowering of VEGF-to-PEDF ratio was significantly correlated with the relief of the vascular damage. It is therefore indicated that the protective effect of ACEI on DR was associated with the decreased VEGF-to-PEDF ratio, which may serve as an effective marker for the development, progression, and treatment outcome of DR.

To further explore the mechanism by which ACEI exerts its protective effect on DR, we investigated the possible role of mitochondrial ROS, which is taken as a key initiator for all of the four pathogenic pathways of diabetic microangiopathy (15–17). We found that high glucose could induce ROS production, which was consistent with our previous study (19); we also noticed that ACEI inhibited

the retinal and cellular production of ROS and blocked the elevation of the VEGF-to-PEDF ratio. We discovered that H_2O_2 upregulated VEGF, downregulated PEDF, and elevated the VEGF-to-PEDF ratio and that NAC, an ROS scavenger, could inhibit hyperglycemia-induced changes of VEGF and PEDF expression and elevation of the VEGF-to-PEDF ratio. These findings suggest that ROS is an upstream molecule of VEGF and PEDF and that ACEI lowers the VEGF-to-PEDF ratio through inhibiting hyperglycemia-induced ROS production.

Hyperglycemia-induced ROS production is primarily thought to be associated with mitochondria and NADPH oxidase (30). A previous study found that both hyperglycemia and angiotensin II, through activating membrane-bound NADH-/NADPH oxidase, could induce superoxide anion generation in human vascular endothelial cells (31). ACEI was also found to inhibit TGF-β and prevent activation of NADPH oxidase so as to attenuate renal damage (32). Mitochondrial ROS was reported to play a very important role in the pathogenesis of DR (16,17,19). Consistent with these studies, our results also revealed that hyperglycemia induced NADPH oxidase activation (data not shown) and mitochondrial membrane hyperpolarization and promoted ROS production. We noticed that perindopril suppressed hyperglycemia-induced activation of NADPH oxidase in a manner similar to that of diphenyleneiodonium in cultured BRECs under hyperglycemic conditions (data not shown).

We discovered, for the first time, that perindopril inhibited the mitochondrial ROS production by increasing the expression of UCP-2, homologous to UCP-1 (33), found in various human tissues, and one of its major functions is as a sensor and negative regulator of ROS production (25). We found that hyperglycemia could compensatorily upregulate UCP-2 so as to negatively modulate $\Delta\psi m$ and ROS because treatment with specific UCP-2 antisense oligonucleotide could increase hyperglycemia-induced mitochondrial membrane hyperpolarization and subsequent ROS generation. We also found that perindopril upregulated UCP-2 and reduced ROS in BRECs exposed to normal glucose, high glucose, or high glucose plus NAC, indicating ACEI can directly upregulate UCP-2; meanwhile, this effect of perindopril could be blocked by the specific UCP-2 antisense oligonucleotide, suggesting that perindopril exerts it effect through UCP-2. It can be concluded that ACEI can attenuate oxidative stress through both the NADPH oxidase pathway and the UCP-2/mitochondrial pathway. In view of the important role of ROS in the pathogenesis DR, the inhibitory effect of ACEI on mitochondrial ROS production might be an important mechanism for treatment of diabetes complications.

We also investigated the specific mechanism by which ACEI induces UCP-2 upregulation and found that PPARγ, a ligand-activated transcription factor belonging to the nuclear receptor superfamily, was involved in the process. PPARγ has two isoforms, γ1 and γ2, and they differ at their NH_2 terminus, which has the same sequence except for the additional 28 amino acids at the NH_2-terminus of PPARγ2. PPARγ2 is rich in the different adipose tissues, whereas PPARγ1 has a broader expression pattern, including the gut, brain, vascular cells, and specific kinds of immune and inflammatory cells (34,35). The measurement of PPARγ protein expression by anti-PPARγ polyclonal antibody could be used to determine the total protein of PPARγ1 and γ2. Owing to its critical role in fat metabolism and the role of PPARγ activators in diabetes prevention, PPARγ has been extensively studied in patients with diabetes (36). It has been reported that PPARγ could benefit vascular function and inhibit neovascularization, retinal leukostasis, and retinal leakage (37–40). Until now, no one has studied the effect of ACEI on PPARγ. Our study is the first to find that perindopril could upregulate PPARγ1 and γ2 in BRECs exposed to normal-glucose or high-glucose conditions; besides, PPARγ inhibitor GW9662 could inhibit the upregulation of UCP-2 expression induced by high glucose or perindopril, suggesting that the upregulation of UCP-2 expression is mediated, at least in part, by PPARγ.

In conclusion, our study suggests that ACEI exerts a protective effect on DR and this protective effect can be reflected by a decreased VEGF-to-PEDF ratio, which is a result of reduced mitochondrial ROS production—itself caused by ACEI-induced increase of PPARγ and subsequent upregulation of UCP-2 expression. It is indicated that ACEI possesses a great potential for treatment of DR; a long-term prospective study based on large samples is needed to verify the clinical effect of ACEI for DR.

ACKNOWLEDGMENTS

This work was supported by grants from the Research Fund for the Doctoral Program of Higher Education of China (20060248077) and the National Nature Science Funding of China (30772370 and 30872828).

No potential conflicts of interest relevant to this article were reported.

We thank Yu Danghui of Second Military Medical University Press for his polishing of the English language.

REFERENCES

1. Ferris FL 3rd, Davis MD, Aiello LM: Treatment of diabetic retinopathy. *N Engl J Med* 341:667–678, 1999
2. Chaturvedi N, Sjolie AK, Stephenson JM, Abrahamian H, Keipes M, Castellarin A, Rogulja-Pepeonik Z, Fuller JH: Effect of lisinopril on progression of retinopathy in normotensive people with type 1 diabetes. The EUCLID Study Group. EURODIAB Controlled Trial of Lisinopril in Insulin-Dependent Diabetes Mellitus. *Lancet* 351:28–31, 1998
3. Neroev VV, Riabina MV, Okhotsimskaia TD, Zueva MV, Tsapenko IV: Use of perindopril in the treatment of patients with diabetic retinopathy. *Vestn Oftalmol* 122:31–33, 2006
4. Gilbert RE, Kelly DJ, Cox AJ, Wilkinson-Berka JL, Rumble JR, Osicka T, Panagiotopoulos S, Lee V, Hendrich EC, Jerums G, Cooper ME: Angiotensin converting enzyme inhibition reduces retinal overexpression of vascular endothelial growth factor and hyperpermeability in experimental diabetes. *Diabetologia* 43:1360–1367, 2000
5. Hogeboom van Buggenum IM, Polak BC, Reichert-Thoen JW, de Vries-Knoppert WA, van Hinsbergh VW, Tangelder GJ: Angiotensin converting enzyme inhibiting therapy is associated with lower vitreous vascular endothelial growth factor concentrations in patients with proliferative diabetic retinopathy. *Diabetologia* 45:203–209, 2002
6. Witmer AN, Blaauwgeers HG, Weich HA, Alitalo K, Vrensen GF, Schlingemann RO: Altered expression patterns of VEGF receptors in human diabetic retina and in experimental VEGF-induced retinopathy in monkey. *Invest Ophthalmol Vis Sci* 43:849–857, 2002
7. Zheng Z, Chen H, Xu X, Li C, Gu Q: Effects of angiotensin-converting enzyme inhibitors and beta-adrenergic blockers on retinal vascular endothelial growth factor expression in rat diabetic retinopathy. *Exp Eye Res* 84:745–752, 2007
8. Patel JI, Tombran-Tink J, Hykin PG, Gregor ZJ, Cree IA: Vitreous and aqueous concentrations of proangiogenic, antiangiogenic factors and other cytokines in diabetic retinopathy patients with macular edema: Implications for structural differences in macular profiles. *Exp Eye Res* 82:798–806, 2006
9. Dawson DW, Volpert OV, Gillis P, Crawford SE, Xu H, Benedict W, Bouck NP: Pigment epithelium-derived factor: a potent inhibitor of angiogenesis. *Science* 285:245–258, 1999
10. Pierce EA, Avery RL, Foley ED, Aiello LP, Smith LE: Vascular endothelial growth factor/vascular permeability factor expression in a mouse model of retinal neovascularization. *Proc Natl Acad Sci U S A* 92:905–909, 1995

11. Gao G, Li Y, Zhang D, Gee S, Crosson C, Ma J: Unbalanced expression of VEGF and PEDF in ischemia-induced retinal neovascularization. *FEBS Lett* 489:270–276, 2001
12. Gao G, Li Y, Fant J, Crosson CE, Becerra SP, Ma JX: Difference in ischemic regulation of vascular endothelial growth factor and pigment epithelium-derived factor in brown Norway and Sprague Dawley rats contributing to different susceptibilities to retinal neovascularization. *Diabetes* 51:1218–1225, 2002
13. Chen H, Jia W, Xu X, Fan Y, Zhu D, Wu H, Xie Z, Zheng Z: Upregulation of PEDF expression by PARP inhibition contributes to the decrease in hyperglycemia-induced apoptosis in HUVECs. *Biochem Biophys Res Commun* 369:718–724, 2008
14. Yang H, Xu Z, Iuvone PM, Grossniklaus HE: Angiostatin decreases cell migration and vascular endothelium growth factor (VEGF) to pigment epithelium derived factor (PEDF) RNA ratio in vitro and in a murine ocular melanoma model. *Mol Vis* 12:511–517, 2006
15. Forbes JM, Coughlan MT, Cooper ME: Oxidative stress as a major culprit in kidney disease in diabetes. *Diabetes* 57:1446–1454, 2008
16. Brownlee M: Biochemistry and molecular cell biology of diabetic complications. *Nature* 414:813–820, 2001
17. Brownlee M: The pathobiology of diabetic complications: a unifying mechanism. *Diabetes* 54:1615–1625, 2005
18. Fiordaliso F, Cuccovillo I, Bianchi R, Bai A, Doni M, Salio M, De Angelis N, Ghezzi P, Latini R, Masson S: Cardiovascular oxidative stress is reduced by an ACE inhibitor in a rat model of streptozotocin-induced diabetes. *Life Sci* 79:121–129, 2006
19. Cui Y, Xu X, Bi H, Zhu Q, Wu J, Xia X, Qiushi R, Ho PC: Expression modification of uncoupling proteins and MnSOD in retinal endothelial cells and pericytes induced by high glucose: the role of reactive oxygen species in diabetic retinopathy. *Exp Eye Res* 83:807–816, 2006
20. Li LX, Yoshikawa H, Egeberg KW, Grill V: Interleukin-1beta swiftly down-regulates UCP-2 mRNA in beta-cells by mechanisms not directly coupled to toxicity. *Cytokine* 23:101–107, 2003
21. Cogan DG, Toussaint D, Kuwabara T: Retinal vascular patterns. IV. Diabetic retinopathy. *Arch Ophthalmol* 66:366–378, 1961
22. Hammes HP, Martin S, Federlin K, Geisen K, Brownlee M: Aminoguanidine treatment inhibits the development of experimental diabetic retinopathy. *Proc Natl Acad Sci U S A* 88:11555–11558, 1991
23. Benani A, Troy S, Carmona MC, Fioramonti X, Lorsignol A, Leloup C, Casteilla L, Pénicaud L: Role for mitochondrial reactive oxygen species in brain lipid sensing: redox regulation of food intake. *Diabetes* 56:152–160, 2007
24. Hassouna A, Loubani M, Matata BM, Fowler A, Standen NB, Galiñanes M: Mitochondrial dysfunction as the cause of the failure to precondition the diabetic human myocardium. *Cardiovasc Res* 69:450–458, 2006
25. Nicholls DG, Locke RM: Thermogenic mechanisms in brown fat. *Physiol Rev* 64:1–64, 1984
26. Kelly LJ, Vicario PP, Thompson GM, Candelore MR, Doebber TW, Ventre J, Wu MS, Meurer R, Forrest MJ, Conner MW, Cascieri MA, Moller DE: Peroxisome proliferator-activated receptors gamma and alpha mediate in vivo regulation of uncoupling protein (UCP-1, UCP-2, UCP-3) gene expression. *Endocrinology* 139:4920–4927, 1998
27. Fukumoto M, Takai S, Ishizaki E, Sugiyama T, Oku H, Jin D, Sakaguchi M, Sakonjo H, Ikeda T, Miyazaki M: Involvement of angiotensin II-dependent vascular endothelial growth factor gene expression via NADPH oxidase in the retina in a type 2 diabetic rat model. *Curr Eye Res* 33:885–891, 2008
28. Wilkinson-Berka JL, Tan G, Jaworski K, Ninkovic S: Valsartan but not atenolol improves vascular pathology in diabetic Ren-2 rat retina. *Am J Hypertens* 20:423–430, 2007
29. Matsuoka M, Ogata N, Minamino K, Higuchi A, Matsumura M: High levels of pigment epithelium-derived factor in the retina of a rat model of type 2 diabetes. *Exp Eye Res* 82:172–178, 2006
30. Coughlan MT, Cooper ME, Forbes JM: Renal microvascular injury in diabetes: RAGE and redox signaling. *Antioxid Redox Signal* 9:331–342, 2007
31. Zhang H, Schmeisser A, Garlichs CD, Plotze K, Damme U, Mugge A, Daniel WG: Angiotensin II-induced superoxide anion generation in human vascular endothelial cells: role of membrane-bound NADH-/NADPH-oxidases. *Cardiovasc Res* 44:215–222, 1999
32. Onozato ML, Tojo A, Kobayashi N, Goto A, Matsuoka H, Fujita T: Dual blockade of aldosterone and angiotensin II additively suppresses TGF-beta and NADPH oxidase in the hypertensive kidney. *Nephrol Dial Transplant* 22:1314–1322, 2007
33. Fleury C, Neverova M, Collins S, Raimbault S, Champigny O, Levi-Meyrueis C, Bouillaud F, Seldin MF, Surwit RS, Ricquier D, Warden CH: Uncoupling protein-2: a novel gene linked to obesity and hyperinsulinemia. *Nat Genet* 15:269–272, 1997
34. Michalik L, Auwerx J, Berger JP, Chatterjee VK, Glass CK, Gonzalez FJ, Grimaldi PA, Kadowaki T, Lazar MA, O'Rahilly S, Palmer CN, Plutzky J, Reddy JK, Spiegelman BM, Staels B, Wahli W: International Union of Pharmacology. LXI. Peroxisome proliferator-activated receptors. *Pharmacol Rev* 58:726–741, 2006
35. Marx N, Bourcier T, Sukhova GK, Libby P, Plutzky J: PPARgamma activation in human endothelial cells increases plasminogen activator inhibitor type-1 expression: PPARgamma as a potential mediator in vascular disease. *Arterioscler Thromb Vasc Biol* 19:546–555, 1999
36. Vinik A, Parson H, Ullal J: The role of PPARs in the microvascular dysfunction in diabetes. *Vascul Pharmacol* 45:54–64, 2006
37. Blaschke F, Spanheimer R, Khan M, Law RE: Vascular effects of TZDs: new implications. *Vascul Pharmacol* 45:3–18, 2006
38. Murata T, Hata Y, Ishibashi T, Kim S, Hsueh WA, Law RE, Hinton DR: Response of experimental retinal neovascularization to thiazolidinediones. *Arch Ophthalmol* 119:709–717, 2001
39. Muranaka K, Yanagi Y, Tamaki Y, Usui T, Kubota N, Iriyama A, Terauchi Y, Kadowaki T, Araie M: Effects of peroxisome proliferator-activated receptor gamma and its ligand on blood–retinal barrier in a streptozotocin-induced diabetic model. *Invest Ophthalmol Vis Sci* 47:4547–4552, 2006
40. Clasen R, Schupp M, Foryst-Ludwig A, Sprang C, Clemenz M, Krikov M, Thone-Reineke C, Unger T, Kintscher U: PPARgamma-activating angiotensin type-1 receptor blockers induce adiponectin. *Hypertension* 46:137–143, 2005